Strojniški vestnik - Journal of Mechanical Engineering 70(2024)1-2, 55-69
DOI:10.5545/sv-jme.2023.709
Original Scientific Paper
Received for review: 2023-06-28
Received revised form: 2023-09-26
Accepted for publication: 2023-09-28

A New Calculation Method for Instantaneous Efficiency and Torque Fluctuation of Spur Gears

Xin Tian[1,2] – Guangjian Wang[1,2,*] – Yujiang Jiang[1,2]

[1] Chongqing University, State Key Laboratory of Mechanical Transmissions, China
[2] Chongqing University, College of Mechanical and Vehicle Engineering, China

As a critical component of the joint gearbox, spur gear pairs play a crucial role in energy conversion, limiting the performance of a collaborative robot. Accurately assessing their instantaneous efficiency and torque fluctuation is essential for developing high-precision robot joint control models. This study proposes a computational model to predict the instantaneous efficiency and torque fluctuation of spur gears under typical operating conditions. The model incorporates a torque balance model, a load distribution model, and a friction model to reflect the relationship between gear meshing position and efficiency. The instantaneous efficiency and torque fluctuation of gear pairs were compared with the Coulomb friction model with an average friction coefficient and the elastohydrodynamic lubrication model with a time-varying friction coefficient. The effect of gear contact ratio on efficiency is analysed, while the instantaneous efficiency and torque fluctuation of gears are studied under varying operating conditions. The results indicate a maximum efficiency difference of 1.86 % between the two friction coefficient models. Under specific operating conditions, the instantaneous efficiency variation of the gear pair can reach 3.34 %, and the torque fluctuation can reach 5.19 Nm. Finally, this study demonstrates the effectiveness and accuracy of the proposed method through comparative analysis.

Keywords: collaborative robot, instantaneous efficiency, torque fluctuation, friction coefficient, load distribution

Highlights

- *A new model to predict instantaneous efficiency and torque fluctuation of spur gears.*
- *The model includes torque balance, load distribution, and friction models.*
- *Instantaneous efficiency of gear pairs is examined under different friction coefficient models.*
- *Torque fluctuation of gear pairs under different friction coefficient models.*
- *Gear efficiency and torque trends are analysed under varying operating conditions.*

0 INTRODUCTION

Collaborative robots are widely used in manufacturing, assembly, rehabilitation, and medical treatment and have become a research hotspot in recent years. To achieve high-precision force/position control of collaborative robots, it is necessary to establish an accurate control model of the joint reducer. However, the commonly used harmonic drive has many disadvantages, such as low efficiency and stiffness, large speed and torque fluctuations, and complex hysteresis characteristics [1] to [3], which directly affect the control precision of collaborative robots. To overcome the limitations of the harmonic drive, many researchers have recently started to study the 3K planetary joint reducer with high efficiency and stiffness to meet the high-precision force/position control requirements of collaborative robots [1] and [4] to [6]. However, these studies mainly focus on efficiency optimization design and less on the research of instantaneous efficiency characteristics. The torque fluctuation caused by instantaneous efficiency will directly affect the control performance of collaborative robots. As the basic transmission unit of the joint reducer, the instantaneous efficiency and torque fluctuation of gear pairs have a direct effect on the stability and lifespan of collaborative robot joints. Therefore, studying the instantaneous efficiency and torque fluctuation characteristics of the gear pair is of great significance for improving the friction characteristics and control model of the joint reducer of collaborative robots.

Energy consumption has drawn much attention in recent years due to the global energy crisis and increasingly stringent environmental regulations. Therefore, improving the efficiency of transmission devices has become an important indicator for evaluating the performance of collaborative robots' joint reducers and other transmission devices in the future [5], and [7] to [9]. In order to accurately evaluate the instantaneous efficiency of planetary gear reducers, it is necessary to study the dynamic changes in the instantaneous efficiency of gear pairs at different meshing positions and contact ratios. As a basic component of planetary transmission systems, the meshing efficiency of gear pairs directly affects the performance of joint reducers in collaborative robots. For example, a 1 % increase in gear meshing

*Corr. Author's Address: Chongqing University, State Key Laboratory of Mechanical Transmissions, Chongqing, 400044, China, gjwang@cqu.edu.cn

efficiency can improve the efficiency of a compound gear train by 30 % [10]. The existing literature focuses more on the average efficiency of gears. When calculating the average efficiency of gear pairs, Höhn [11] introduced a loss factor based on the Coulomb friction model, considering the influence of gear geometry. Baglioni et al. [12] analysed the effects of different friction coefficient calculation models, transmission ratios, addendum modification coefficients, loads, and speeds on the average efficiency of gear pairs. Pleguezuelos et al. [13] calculated the average efficiency of gear pairs based on a load distribution model and a friction model that remained constant along the contact path and studied the effects of transmission ratio and pressure angle on efficiency. Marques et al. [14] investigated the effects of rigid and elastic load distribution models on the average efficiency of gear pairs while analysing the average power loss of gears under local and constant friction coefficients. Diez-Ibarbia et al. [15] proposed an average efficiency evaluation model for gear pairs that simultaneously considers the Coulomb friction model and load distribution and analysed the effects of addendum modification coefficient, different friction coefficient calculation formulas [16], and tooth profile modification [17] on gear efficiency. Petry-Johnson et al. [18] analysed the changing trends of the average meshing efficiency of gear transmission systems and the average efficiency of gearboxes under different speeds and load torque through experiments.

The instantaneous efficiency of a compound gear train can vary by more than ±20 % from the average efficiency [19], while there are relatively few studies on the instantaneous efficiency of gear pairs. Cao et al. [20] found that the instantaneous efficiency variation of bevel gears can reach up to 8 %. Li and Kahraman [21] proposed a model for predicting the mechanical power loss related to a load of a gear pair based on the elastohydrodynamic lubrication (EHL) theory. The model predicts the instantaneous mechanical power loss at each tooth contact and the overall power loss at gear engagement based on the pressure and film thickness of the lubricating oil. However, this model is analytically difficult, neglects the load distribution between the teeth, and cannot be used to investigate the torque fluctuation of gear pairs. Xu et al. [22] modelled the time-varying friction coefficient (TFC) at the gear contact point to predict the mechanical power loss caused by gear friction, and analysed the effects of geometric parameters, tooth profile modifications, operating conditions, surface roughness, and lubricant performance on mechanical efficiency loss. However, they only calculated the average efficiency without delving into the instantaneous efficiency in depth. Wang et al. [19] proposed a method for analysing instantaneous efficiency using a load distribution model. However, this method cannot accurately evaluate the instantaneous efficiency of gears and ignores the relationship between the instantaneous efficiency of gear pairs and torque fluctuation. Therefore, there is an urgent need to propose a calculation model that can accurately evaluate the instantaneous efficiency of gear pairs.

In studying the instantaneous transmission efficiency of gear pairs under constant speed and load, it is generally desirable to have a stable torque for the output side shafting [9]. The strong nonlinearity and time-varying nature of internal friction characteristics in gear pairs cause torque fluctuation not only to vary with the meshing position of the gears but also to be affected by various factors, such as operating temperature [9], [23], and [24], load torque [18], and contact surface roughness [25]. These fluctuations reduce system stability, leading to significant noise and vibration problems [26]. At present, many scholars have carried out modelling and compensation studies on the friction torque of robot harmonic reducers. Lu et al. [27] proposed a method to compensate for the torque fluctuation of a harmonic reducer by using a torque sensor. Tadese et al. [24] used a dynamic friction model that considers temperature fluctuations to predict the joint torque variations of a collaborative robot mechanical arm driven by a harmonic reducer. Although the torque fluctuation and friction model of harmonic reducers have been extensively studied, there are relatively few studies on the torque fluctuation of gear pairs. For collaborative robots employing 3K planetary transmissions, an in-depth investigation into their friction models and torque fluctuations is crucial for achieving precise force and position control. Therefore, studying the torque fluctuations of gear pairs is essential in enhancing the accuracy and reliability of the system. Accurately assessing torque fluctuations in gear pairs is crucial to improving the accuracy and reliability of a system.

In summary, this paper proposes a computational model for predicting the instantaneous efficiency and torque fluctuation of gear pairs, considering the torque balance at the meshing point, the load distribution between teeth, and the friction coefficient models. The instantaneous efficiency and torque fluctuation of gear pairs under the average friction coefficient (AFC) based on Coulomb friction and the TFC based on EHL are compared. Additionally, the relationship between gear instantaneous efficiency and torque fluctuation is analysed, and the influence of contact ratio on

efficiency is discussed. Compared with existing research, which mainly focuses on the influence of output torque and speed on the average efficiency of gears [12], [15] to [17], and [28], this paper not only considers load and speed conditions but also explores the influence of surface roughness and lubricating oil operating temperature on the instantaneous efficiency and torque fluctuation of gears. Finally, the effectiveness and accuracy of the proposed method were verified through comparative analysis.

The paper is organized as follows. Section 1 develops a model for calculating the instantaneous efficiency of gears based on the torque balance, load distribution model, and friction coefficient model. Section 2 presents a study on the instantaneous efficiency and torque fluctuation of gears under different friction coefficient models with given parameters (geometric parameters and operating conditions). Section 3 discusses the evaluation results of gear efficiency and torque fluctuation under four operating conditions, validating the effectiveness and accuracy of the proposed method. Section 4 is the research conclusion.

1 METHODS

1.1 Instantaneous Efficiency Model of Gears

In gear transmission, it has been found through numerous experiments and numerical analyses that load-dependent power losses are the main cause of changes in system efficiency [11], [16], [18], and [28]. In addition, losses due to sliding friction under adverse load conditions account for approximately 95 % of the losses [17]. Therefore, this paper focuses on the effect of sliding friction on the instantaneous efficiency of gears. To determine the instantaneous efficiency of gears, it is crucial to have a comprehensive understanding of the meshing process; for gears with a contact ratio between 1 and 2, they will sequentially cross the double-tooth meshing area, single-tooth meshing area, and double-tooth meshing area as they mesh in and out along the actual meshing line B_1B_2. Fig. 1 describes the three key moments of the meshing of a pair of gear wheels with a contact ratio between 1 and 2. There are three pairs of gears involved in the entire meshing process in a single cycle from the in-mesh to the out-mesh. Fig. 1a shows gear pair 2 meshing in the double-tooth meshing area B_1B_{lpstc} while gear pair 3 meshes out in the double-tooth meshing area $B_{hpstc}B_2$. At this time, there are two meshing points on the meshing line B_1B_2. Fig. 1b shows the situation of gear pair 2 entering the

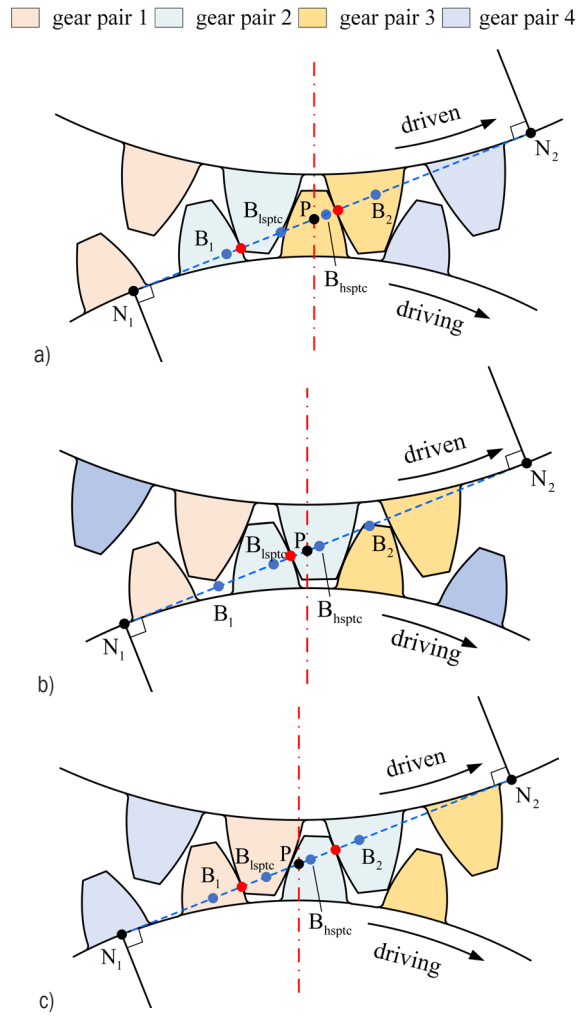

Fig. 1. *Gear meshing process; a) MMGP in double-tooth meshing area B1Blsptc b) MMGP in single-tooth meshing area BlsptcBhsptc, and c) MMGP in double-tooth meshing out area*

single-tooth meshing area $B_{lpstc}B_{hpstc}$ from the double-tooth meshing area B_1B_{lpstc}. At this time, there is only one meshing point in the meshing area B_1B_2. Fig. 1c shows gear pair 2 entering the double-tooth meshing rea $B_{hpstc}B_2$ while gear 1 meshes in the double-tooth meshing area B_1B_{lpstc}. There are two meshing points on the meshing line B_1B_2, and gear pair 2 gradually exits the meshing area, completing one gear meshing cycle. For ease of discussion, the gear pair that completes one gear meshing cycle on the meshing line B_1B_2 is defined as the main meshing gear pair (MMGP), such as gear pair 2 mentioned above. When the MMGP is in the double-tooth meshing area, other gear pairs participating in the meshing process are defined as secondary meshing gear pairs (SMGP). It should be noted that there are two gear pairs in the SMGP during

a single gear meshing cycle of the MMGP, such as gear 3 when gear pair 2 appears in B_1B_{lpstc} and gear pair 1 when gear pair 2 appears in $B_{hpstc}B_2$.

When calculating the instantaneous efficiency of the gear pair along the line of contact, the torque balance at different mesh positions, load distribution between teeth, and friction coefficients must be considered. The force analysis of the gear along the contact line is shown in Fig. 2, where P is the meshing node, N_1N_2 is the theoretical contact line, B_1B_2 is the actual contact line, and K_1 and K_2 are the meshing points of the gear profiles of the MMGP and SMGP during the gear transmission process, respectively. The input torque of the driving gear is defined as positive, and the output torque of the driven gear is defined as negative. The gear friction torque is not always in the same direction because the direction of the sliding velocity of the contact point changes up and down at the node, which causes the direction of the friction torque to change. In addition, in the double-tooth meshing area, the parameters such as contact force, sliding velocity, and curvature radius of different meshing points are different, so the friction coefficient and load distribution of each meshing point must be considered separately.

Based on the torque balance model at the meshing point, load distribution between teeth, and friction coefficient, this paper proposes the instantaneous efficiency calculation model for gears. The instantaneous input torque of the gear in the double-tooth meshing area at any moment is expressed as follows:

$$\begin{aligned} T_{\text{in}} &= F_n R_{b1} \pm \lambda \mu_1 F_n R_{b1} \tan \alpha_{K1} \\ &\mp (1-\lambda)\mu_2 F_n R_{b1} \tan \alpha_{K2}, \end{aligned} \tag{1}$$

where F_n is the contact force, R_{b1} is the base circle radius of the driving gear, λ is the load distribution factor (be discussed in a subsequent section), μ_1 and μ_2 are the friction coefficients of MMGP and SMGP, respectively (to be discussed in a subsequent section), α_{K1} and α_{K2} are the instantaneous meshing positions of MMGP and SMGP on the driving gear, respectively.

The output torque of the gear at any instant in the double-tooth meshing area are as follows:

$$\begin{aligned} T_{out} &= -F_n R_{b2} \mp \lambda \mu_1 F_n R_{b2} \tan \beta_{K1} \\ &\pm (1-\lambda)\mu_2 F_n R_{b2} \tan \beta_{K2}, \end{aligned} \tag{2}$$

where R_{b2} is the base circle radius of the driven wheel, β_{K1} and β_{K2} are the instantaneous meshing positions of MMGP and SMGP on the driven wheel, respectively.

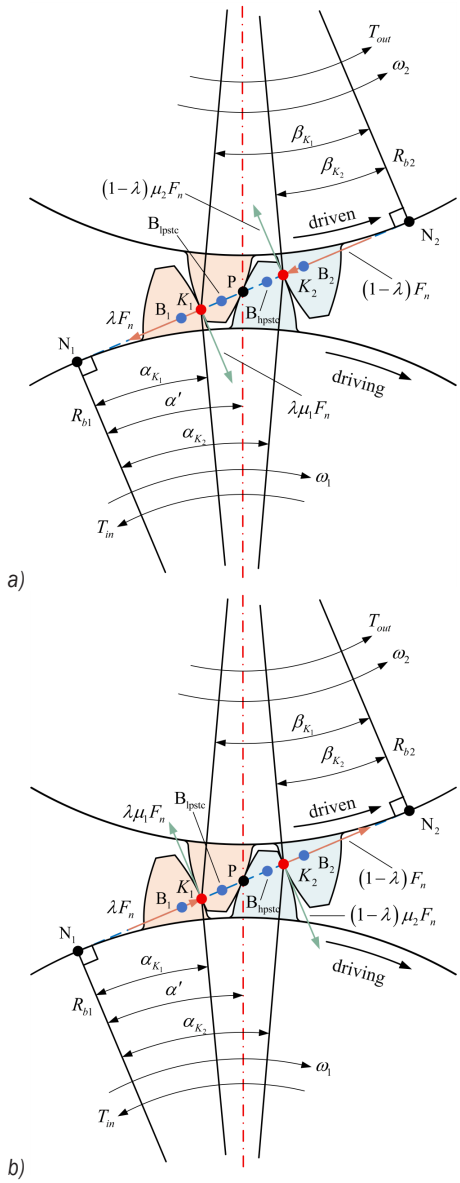

Fig. 2. *Gear force analysis; a) forces and friction on a driving gear, and b) forces and friction on a driven wheel*

In summary, the instantaneous efficiency calculation model of the gear is Eq. (3):

$$\begin{aligned} \eta &= -\frac{T_{out}\omega_2}{T_{in}\omega_1} \\ &= \begin{cases} \dfrac{1-\lambda\mu_1\tan(\beta_{K1})+(1-\lambda)\mu_2\tan(\beta_{K2})}{1-\lambda\mu_1\tan(\alpha_{K1})+(1-\lambda)\mu_2\tan(\alpha_{K2})}, \\ \text{when} \quad 0 < B_1K_1 < B_1P \\ \dfrac{1+\lambda\mu_1\tan(\beta_{K1})-(1-\lambda)\mu_2\tan(\beta_{K2})}{1+\lambda\mu_1\tan(\alpha_{K1})-(1-\lambda)\mu_2\tan(\alpha_{K2})}, \\ \text{when} \quad B_1P < B_1K_1 < B_1B_2 \end{cases} \end{aligned} \tag{3}$$

where $B_1K_1 = R_{b1}\tan\alpha_{K1} - N_1B_1$, ω_1 and ω_2 are the angular velocity of the driving and driven wheel. When $B_1P < B_1K_1 < B_1B_{1hsptc}$, it is the instantaneous efficiency of single-tooth meshing area.

In addition to the above method of using torque balance to obtain the instantaneous efficiency of the gear, the efficiency of the gear can also be obtained through the friction power loss of the gear. The calculation of load-dependent power losses in gear is based on Coulomb friction Eq. (4):

$$F_R = \mu F_N \tag{4}$$

$$P_{loss} = F_R V_g = \mu F_N V_g, \tag{5}$$

where P_{loss} is power loss, μ is coefficient of friction, F_N is normal force, V_g is sliding speed.

Eq. (5) calculates the friction power loss of the gear only for a single-point contact [11], ignoring the alternate meshing process of single and double teeth and leading to an inaccurate evaluation of the power loss over one meshing cycle. Based on the concept presented in this section, this paper modifies Eq. (5) considering the load distribution between gear teeth at the double-tooth meshing position, as well as the friction coefficient and sliding velocity, to obtain the instantaneous friction power loss of the gear is as follows:

$$P_{loss,i} = F_{n,i}\left|\lambda_i\mu_{1,i}v_{s_1,i} - (1-\lambda_i)\mu_{2,i}v_{s_2,i}\right|. \tag{6}$$

The calculation model of average friction loss power is as follows:

$$P_{\text{loss}} = \frac{F_{n,i}}{B_1B_2}\left(\begin{array}{l}\int_{B_1}^{B_{lsptc}}\left|\lambda_i\mu_{1,i}v_{s_1,i} - (1-\lambda_i)\mu_{2,i}v_{s_0,i}\right|dx \\ +\int_{B_{lsptc}}^{B_{hsptc}}\left|\lambda_i\mu_{1,i}v_{s_1,i}\right|dx \\ +\int_{B_{hsptc}}^{B_2}\left|\lambda_i\mu_{1,i}v_{s_1,i} - (1-\lambda_i)\mu_{2,i}v_{s_2,i}\right|dx\end{array}\right). \tag{7}$$

In this paper, a novel average friction loss calculation model is proposed. Eq. (7) is related not only to the gear parameters themselves but also to the sliding velocity, load, and friction coefficient at the gear meshing point. More importantly, based on the dynamic process of gear on the meshing line, the coupling relationship between different meshing points is considered, and the loss power of single and double teeth meshing is separated. Finally, the gear efficiency is Eq. (8):

$$\eta = \frac{P_{out}}{P_{out} + P_{loss}}. \tag{8}$$

Combining Eqs. (6) and (8), the instantaneous efficiency calculated from the equations is consistent with the result obtained from Eq. (3), which mutually validates the two proposed models for calculating instantaneous efficiency. To facilitate comparison and highlight the instantaneous fluctuation, the terms "average efficiency $\bar{\eta}$" and "efficiency fluctuation $\tilde{\eta}$" will be used to represent the instantaneous efficiency variation of the gear in the subsequent text, while the terms "average input torque $\bar{T}_{in}$" and "torque fluctuation $\tilde{T}_{in}$" will be used to replace the influence of the gear's instantaneous input torque. Efficiency fluctuations $\tilde{\eta}$ and torque fluctuations $\tilde{T}_{in}$ are defined as follows:

$$\tilde{\eta} = \eta_{\max} - \eta_{\min}, \tag{9}$$

$$\tilde{T}_{in} = T_{in\_\max} - T_{in\_\min}, \tag{10}$$

where $\eta_{\max}$ and $T_{in\_\max}$ are the maximum value of instantaneous efficiency and instantaneous input torque, $\eta_{\min}$ and $T_{in\_\min}$ are the minimum value of instantaneous efficiency and instantaneous input torque.

1.2 Load Distribution Coefficient Considering Hertz Contact Stiffness

From Eq. (6), it can be seen that the factors affecting the instantaneous friction power loss of the gear include the contact force, load distribution coefficient, and friction coefficient. The load distribution between the teeth of spur gears is not distributed evenly but is closely related to the contact stiffness at the contact point. In this paper, the load distribution coefficient adopts a widely accepted simplified linear calculation model proposed in [29], as follows:

$$\lambda = \begin{cases} 0.36 + \dfrac{0.28}{\varepsilon_\alpha - 1}B_1K_1, \\ \quad \text{when } 0 < B_1K_1 < B_1B_{\text{lsptc}} \\ 1, \quad \text{when } B_1B_{\text{lsptc}} < B_1K_1 < B_1B_{\text{hsptc}}, \\ 0.36 - \dfrac{0.28}{\varepsilon_\alpha - 1}(B_1K_1 - \varepsilon_\alpha), \\ \quad \text{when } B_1B_{\text{hsptc}} < B_1K_1 < B_1B_2 \end{cases} \tag{11}$$

where ε_α is contact ratio, $1 \le \varepsilon_\alpha \le 2$.

This model uses a linear function to represent the relationship between the load distribution coefficient in two double-tooth meshing areas and the displacement of the meshing point, with a simple calculation process, a small amount of computation, and accurate results. The maximum error between the calculation results of this model and the finite element simulation results is within 6 %.

1.3 Average Friction Coefficient and Time-Varying Friction Coefficient Models

The friction coefficient is an indispensable factor in evaluating the efficiency of gears, and it is a function of many variables [30], such as normal load, sliding velocity, relative curvature radius, surface roughness, oil viscosity, sliding-to-rolling ratio, and temperature. The selection of the friction coefficient greatly affects the accuracy of the gear efficiency calculation. This section will focus on the average friction coefficient and time-varying friction coefficient used in the calculation of instantaneous efficiency and torque fluctuation.

1.3.1 Method I: Average Friction Coefficient

As the coefficient of friction only changes slightly with the variable operating conditions on the path of contact, it can be assumed to be constant for approximation purposes. In this paper, the most commonly used average friction coefficient in the international standard [31] is as follows:

$$\mu_{AFC} = 0.048\left(\frac{F_{\mathrm{bt}}/\mathrm{b}}{v_{\Sigma C}\rho_{\mathrm{red}C}}\right)^{0.2}\eta_{oil}^{-0.05}Ra^{0.25}X_L. \quad (12)$$

1.3.2 Method II: Time-varying Coefficient of Friction

The friction coefficient calculation formula proposed by Xu et al. [22] under EHL conditions was adopted in this study. This formula was obtained by performing multivariate linear regression analysis on a large number of EHL predictions under various contact conditions. Compared to traditional methods, this formula is simpler to calculate, and the calculated friction coefficient based on the EHL formula matches well with the measured traction data. The calculation equation is as follows:

$$\mu_{TFC} = \mathrm{e}^{f(SR,P_h,v_0,S)}P_h^{b_2}\left|SR\right|^{b_3}V_e^{b_6}v_0^{b_7}R^{b_8}, \quad (13)$$

$$f\left(SR,P_h,v_0,S\right) = b_1 + b_4\left|SR\right|P_h\log_{10}\left(v_0\right) + b_5e^{-|SR|P_h\log_{10}(v_0)} + b_9e^{S}. \quad (14)$$

1.4 Calculation of Gear Contact Force Based on Torque Balance Method

When calculating the gear transmission efficiency under constant speed and load, if the friction effect is ignored, the maximum contact force of the gear can be obtained by Eq. (15). The contact force acts on the contact point with a constant direction relative to the rotation axis of the meshing gear, the friction force acts on the tangent surface of the meshing tooth flank, and the friction coefficient is a function of the contact force. Therefore, there is a coupling relationship between the friction coefficient and the contact force, and their numerical changes will affect each other. However, Eq. (15) cannot reflect this relationship. Therefore, in efficiency calculation, the gear contact force and friction coefficient are still the focus of discussion [30]. In this paper, the balance between input torque, output torque, and friction torque at the gear meshing point is considered as the entry point. Through the torque balance method, it establishes the relationship expression between output torque, friction coefficient, and contact force, and solves and calculates the contact force of each meshing point of the gear. This is achieved through an iterative process to calculate the torque generated by contact force and friction force and make them equal to the output torque applied to the system.

$$F_{n\max} = \frac{2T_{out}}{d_2}. \quad (15)$$

For the force analysis of the driven gear under constant speed and load conditions, as shown in Fig. 2, after balancing the output torque, the magnitude of the contact force acting on the contact point is derived from Eq. (2):

$$F_n = \frac{T_{out}}{\left(-1\mp\lambda\mu_1\tan\beta_{K_1}\pm\left(1-\lambda\right)\mu_2\tan\beta_{K_2}\right)R_{b2}}. \quad (16)$$

Since the friction coefficient μ_1 and μ_2 are function of the contact force, the contact force F_n during the gear meshing process cannot be directly obtained from this formula when the gear output torque is known. Therefore, this paper uses a numerical iteration method to solve for the contact force F_n and Eq. (15). is set as the initial value of the contact force F_n iteration.

Set the iteration termination condition as follows:

$$\left|F_{n(i+1)} - F_{n(i)}\right| \le \varepsilon, \quad (17)$$

where $\varepsilon = 0.001$ is the convergence accuracy, and i is the iteration number.

To describe the variation of contact force along the contact line under different friction coefficients visually, the ratio of the contact force for different models to the maximum contact force obtained without considering friction is compared. The ratio of the contact forces obtained from different models after

torque balance is calculated using Eq. (18), and the result is shown in Fig. 5.

$$\beta = \frac{F_{ni}}{F_{n\max}}. \tag{18}$$

2 CASE OF APPLICATION

The specific calculation process is shown in Fig. 3. The parameters of the spur gear are shown in Table 1, the 75W90-A lubricating oil parameters in reference [32], and the operating conditions are shown in Table 2. Under the same operating conditions, the inter-tooth friction coefficients obtained by considering different friction coefficient calculation models and satisfying the torque balance condition from meshing to disengagement for one cycle of MMGP are shown in Fig. 4. In the single-tooth meshing area $B_{lpstc}B_{hpstc}$, the time-varying friction coefficient in Method II quickly decreases to 0 as MMGP approaches node P and increases as MMGP moves away from node P. This is a clear local variation process, while the average friction coefficient calculated by Method I in this area is almost a straight line and a constant value. In other double-tooth meshing areas, the value of the time-varying friction coefficient is significantly larger than that of the average friction coefficient. The friction coefficient of SMGP only exists in the double-tooth meshing area, which is due to the different gears involved in the meshing and disengagement processes.

Considering the friction and torque balance, the ratio of the contact forces of the MMGP along the actual contact line is shown in Fig. 5 at different meshing positions. In the double-tooth meshing area B_1B_{lpstc} of the SMGR, the contact force is proportional to the meshing distance, while in the double-tooth meshing area $B_{hpstc}B_2$, the change in contact force is opposite to the trend in the B_1B_{lpstc} meshing area and is inversely proportional to the meshing distance. At this time, MMGP is in the meshing-out process, and the load is gradually borne by SMGR. In these two double-tooth meshing areas, the contact force obtained by Method I is greater than the contact force without friction, and the contact force obtained by Method II is greater than that obtained by Method I. These three methods are almost identical in size when entering the double-tooth meshing area, and the difference between them becomes significant as the double-tooth meshing distance increases. At the points B_{lpstc} and B_{hpstc}, the contact force of the gear pair will produce a step change because the gear pair undergoes a single-double tooth meshing transition, which will cause impact and vibration at this moment.

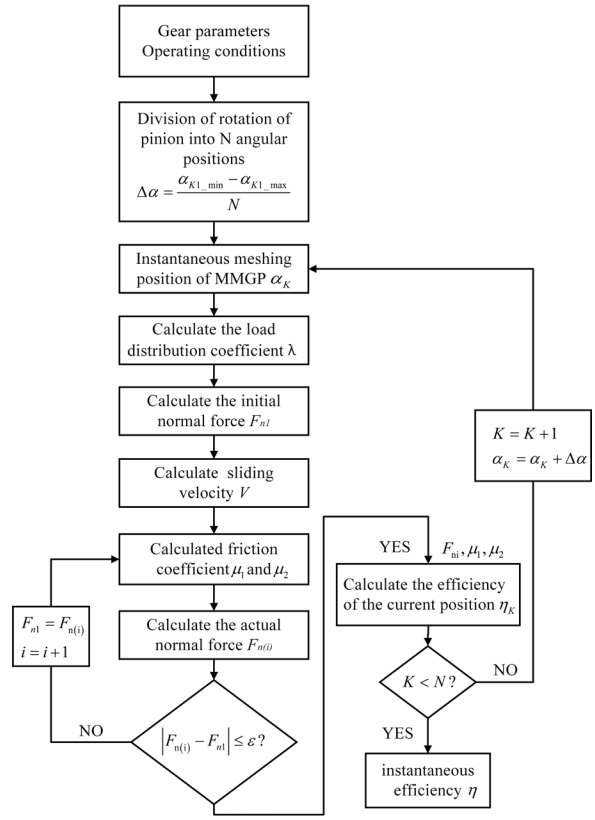

Fig. 3. *The calculation flowchart of the mathematical model of the gear instantaneous efficiency model*

Table 1. *Pinion/gear parameters*

Parameters	
Teeth number of pinion	$Z_1 = 18$
Teeth number of wheel	$Z_2 = 36$
Pressure angle [°]	$\alpha = 20$
Helix angle [°]	$\beta = 0$
Module [mm]	$m = 3$
Face width [mm]	$b = 26.7$
Centre distance [mm]	$a = 81$
Transverse contact ratio	$\varepsilon_\alpha = 1.611$

Table 2. *Operating conditions*

Operating conditions	Output torque T_{out} [Nm]	Input speed n_1 [rpm]	Surface roughness Ra [μm]	Lubricant operating temperature θ_{oil} [°C]
case 1	159	1500	0.8	55
case 2	Δ	1500	0.8	55
case 3	159	Δ	0.8	55
case 4	159	1500	Δ	55
case 5	159	1500	0.8	Δ

Symbol Δ: this value will change in Section 3.

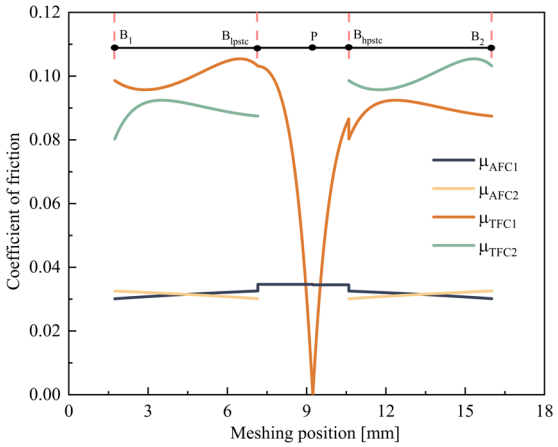

Fig. 4. *The friction coefficient of the gear pair at case 1: μ_{AFC1} and μ_{TFC1} are the friction coefficients of MMGP at different meshing positions, μ_{AFC2} and μ_{TFC2} are the friction coefficients of SMGR in the double-tooth meshing area*

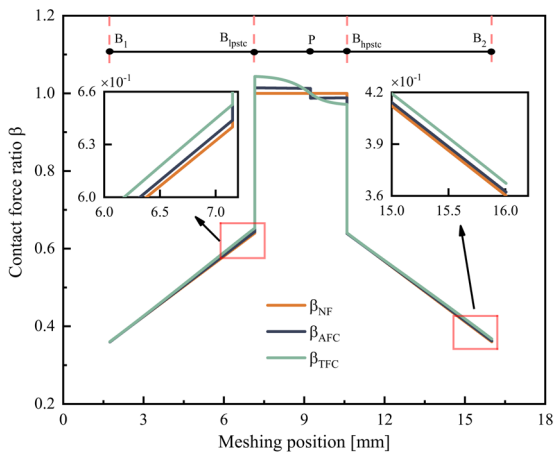

Fig. 5. *The ratio of the contact force of the MMPG gear during the engagement cycle at case 1: without friction (β_{NF}), with average friction coefficient (β_{AFC}), and with time-varying friction coefficients (β_{TFC})*

In the single-tooth meshing area $B_{lpstc}B_{hpstc}$, the contact force obtained by Method I undergoes a sudden change at node P. The reason for this phenomenon is that the sliding velocity direction of the meshing points on the left and right of node P changes, and the frictional force is related to the sliding velocity which leads to a change in the direction of the frictional torque before and after the node. The contact force obtained by Method II in the single-tooth meshing area will decrease smoothly with the meshing position and will not produce a jump phenomenon. The phenomenon in Fig. 5 is consistent with the previous research **[15]** to **[17]**. It can be seen that the size of the tooth surface contact force calculated by different friction coefficient calculation models is different.

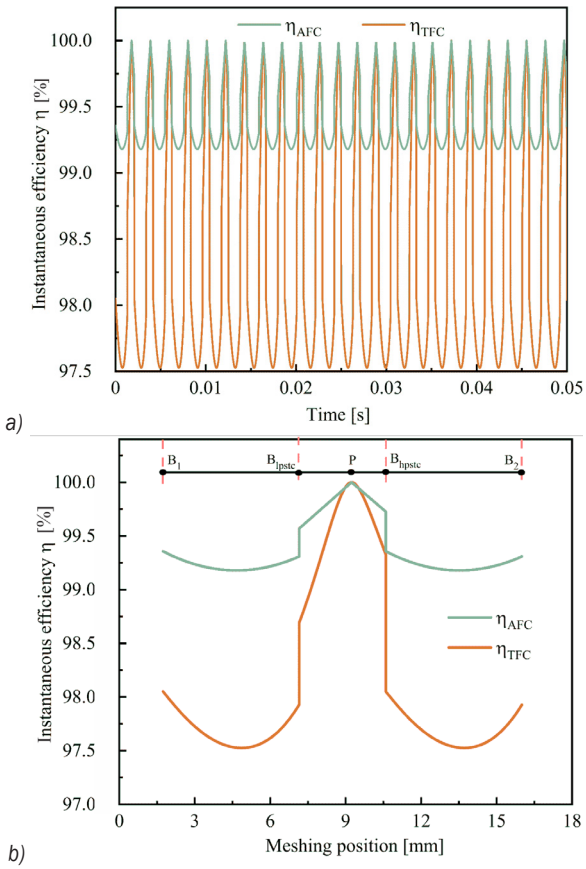

Fig. 6. *Gear instantaneous efficiency at case 1: a) The variation of instantaneous efficiency with time in the gear meshing process, b) Instantaneous efficiency at one meshing cycle, η_{AFC} is the instantaneous efficiency obtained by Method I, η_{TFC} is the instantaneous efficiency obtained by Method II*

The instantaneous meshing efficiency of the gear under different friction coefficient calculation methods is shown in Fig. 6. Fig. 6a represents the change in the instantaneous efficiency of the gear over time. The instantaneous meshing efficiency obtained by Method I (η_{AFC}) changes from 99.18 % to 100 %, and the fluctuation range of instantaneous efficiency is 0.82 %. The instantaneous meshing efficiency obtained by Method II (η_{TFC}) changes from 97.53 % to 100 %, and the fluctuation range of instantaneous efficiency is 2.47 %. At the same time, the value of η_{TFC} is lower than the value of η_{AFC} at the same meshing position. Fig. 6b can more clearly reflect the instantaneous meshing efficiency of the gear at any meshing point on the meshing line. Regardless of η_{AFC} or η_{TFC}, there will be a significant abrupt change in instantaneous efficiency in the process of single-to-double tooth alternation. At the double-tooth meshing area, the instantaneous efficiency is lower than that in the single-tooth meshing area. This is because the

relative sliding velocity generated by the gear in the double-tooth meshing area is greater than that in the single-tooth meshing area. The instantaneous meshing efficiency at node P is the highest. Although different methods have different friction coefficients at the nodes, the same results can be obtained. For η_{TFC}, there is no relative sliding between the driving and driven wheels at the node, and the friction coefficient is 0, so the efficiency is the highest. For η_{AFC}, although the friction coefficient at the node is not 0, the actual meshing angle at the node is the same, which produces the same result as η_{TFC}. This explains why the numerical values of the different friction coefficient models are different at the node, but their instantaneous efficiency is consistent.

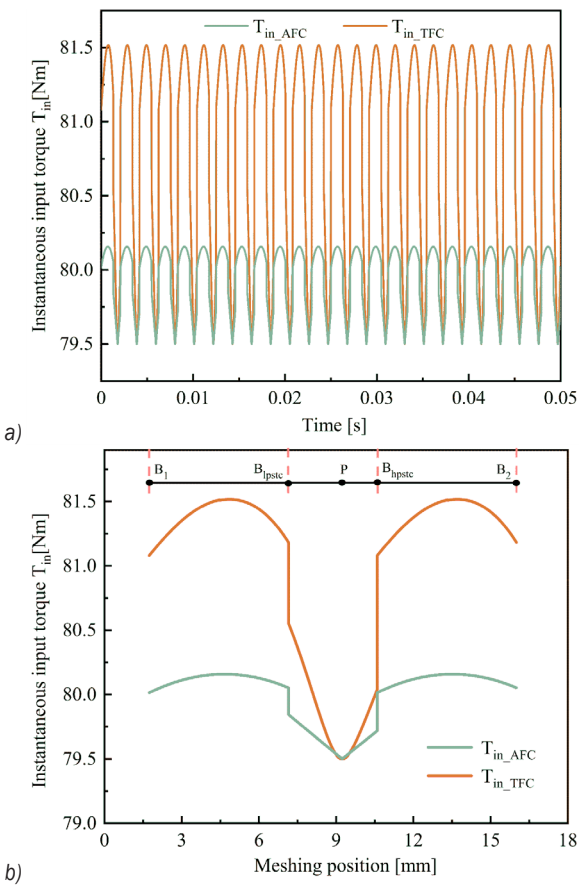

Fig. 7. *Gear instantaneous input torque at case 1: a) the variation of instantaneous input torque with time in gear meshing process; b) Instantaneous input torque at one meshing cycle, T_{in_AFC} is the instantaneous input torque obtained by Method I, T_{in_TFC} is the instantaneous input torque obtained by Method II*

Under constant speed and load conditions, where a constant output torque is maintained on the driven gear, the instantaneous input torque of the driving gear fluctuates due to the existence of tooth friction and changes in the meshing position, as shown in Fig. 7. Fig. 7a shows the variation of the instantaneous input torque with time, with T_{in_AFC} changes from 79.50 Nm to 80.16 Nm with a torque fluctuation range of 0.66 Nm, and T_{in_TFC} changes from 79.50 Nm to 80.52 Nm with a torque fluctuation range of 2.02 Nm. Fig. 7b shows the variation of the instantaneous input torque with the meshing position of the gear, where the instantaneous input torque in the double-tooth meshing area is higher than that in the single-tooth meshing area, and T_{in_TFC} is higher than T_{in_AFC} at the same meshing position. Method I has a smaller torque fluctuation than Method II.

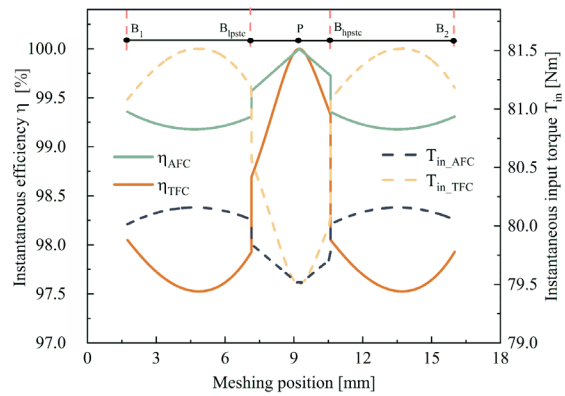

Fig. 8. *The instantaneous efficiency and instantaneous input torque of the gear at case 1*

Fig. 8 shows that the instantaneous efficiency of the gear decreases as the instantaneous input torque increases. The greater the fluctuation in gear efficiency, the greater the resulting torque fluctuation. The increase in input torque fluctuation not only reduces stability but also creates significant noise and vibration problems, making it difficult to model and compensate for. This also poses a challenge to the original engine. Without changing the gear ratio, increasing the proportion of single-tooth meshing in the actual meshing area, i.e., reducing the contact ratios of the gear, can improve gear transmission efficiency and reduce torque fluctuation. Fig. 9 shows the average efficiency and the efficiency fluctuation of the gear for different contact ratios, showing that decreasing the contact ratio can improve the gear efficiency. However, it should be noted that reducing the gear contact ratio also affects gear transmission capacity, load capacity, and service life. Therefore, in practical applications, a balance and selection should be made based on specific circumstances, ensuring continuous gear transmission while minimizing contact ratio to achieve maximum gear efficiency.

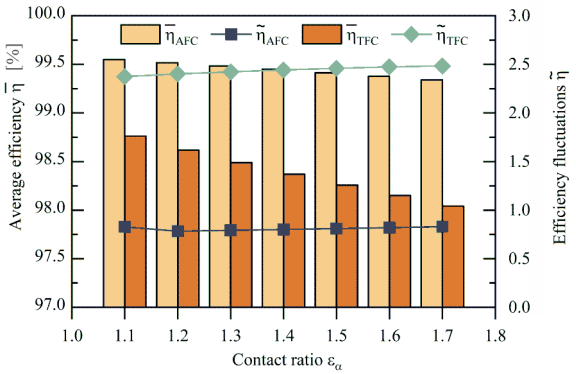

Fig. 9. *Influence of gear contact ratio at case 1 on efficiency*

3 RESULTS

The efficiency of a gear pair is not only related to factors such as friction coefficient and tooth load distribution but also to operating conditions. Previous research has focused on the effects of friction coefficient calculation models, gear ratios, addendum modification coefficients, loads, and speeds on gear efficiency **[12]**, **[15]**, and **[16]**, neglecting the effects of gear surface roughness and lubricant operating temperature on gear efficiency and lacking exploration of the effects of different operating conditions on torque fluctuations during gear meshing. Improper design of gear surface roughness and lubricant operating temperature can lead to more friction power loss, reducing gear meshing efficiency and increasing input torque fluctuation. This section focuses on the variability of gear efficiency and torque fluctuations under four different operating conditions: different output torque, input speed, gear surface roughness, and lubricant operating temperature.

3.1 Gear Instantaneous Efficiency under Different Operating Conditions

The meshing efficiency and efficiency fluctuation for gears under different operating conditions are shown in Fig. 10. $\bar{\eta}_{AFC}$ and $\bar{\eta}_{TFC}$ represent the average efficiency under Method I and Method II, respectively. $\tilde{\eta}_{AFC}$ and $\tilde{\eta}_{TFC}$ represent the instantaneous efficiency fluctuation under Method I and Method II, respectively. Fig. 10a shows the influence of different output torques on the average efficiency and efficiency fluctuation. The average efficiency obtained by Method I decreases as the input torque increases, while Method II shows the opposite trend. The difference in the results obtained by the two methods is mainly due to the fact that the friction coefficient calculation formula in Method I increases with the increase of the output torque, causing an increase in

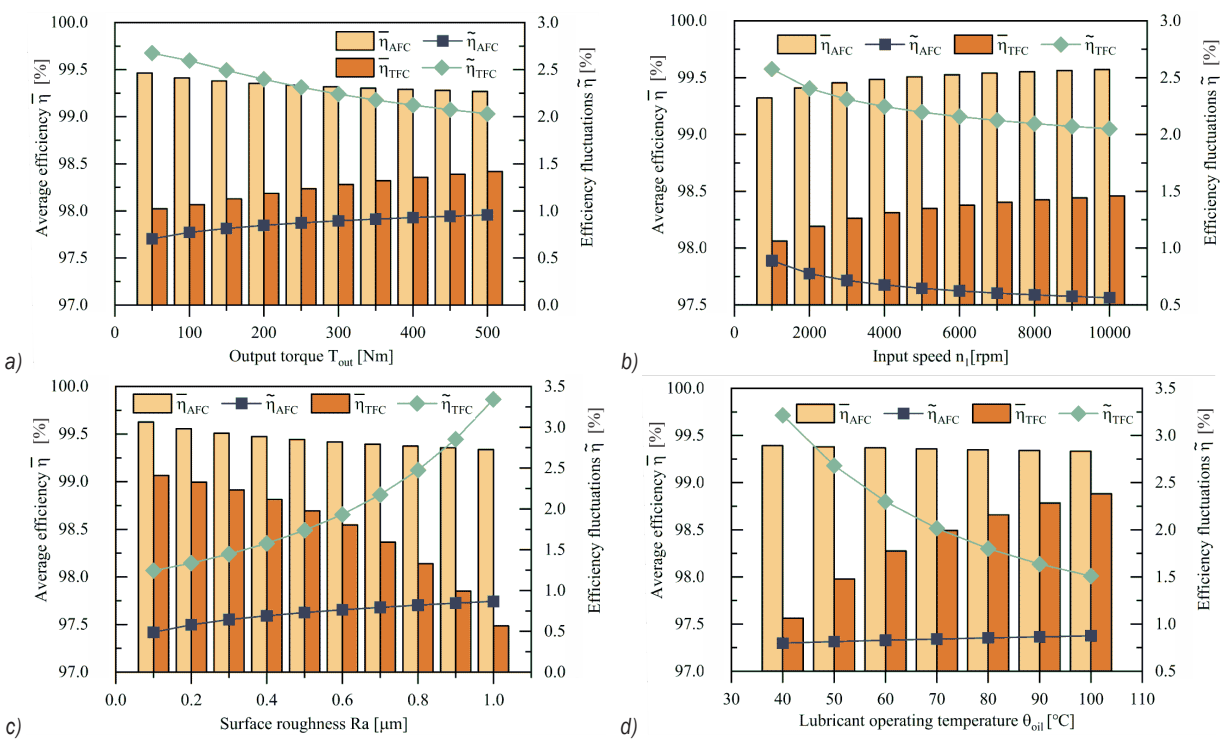

Fig. 10. *Efficiency and efficiency fluctuation of gears; a) at case 2, b) at case 3, c) at case 4, and d) at case 5*

frictional losses, resulting in a decrease in efficiency. However, the effect of the efficiency decrease is not significant, only 0.19 %. In contrast, the friction coefficient formula in Method II results in a decrease in instantaneous friction coefficient with the increase of the output torque, resulting in a decrease in frictional losses and an increase in efficiency. The amplitude of the efficiency fluctuation is greater than that of the efficiency obtained by Method I. The difference in gear meshing efficiency values obtained by the two methods is at most 1.44 %. The main reason for the difference in calculation results is that the friction coefficient at each contact point in Method II is a local variable that varies with time, while the friction coefficient in Method I is an average value along the contact line. The effect of input speed on gear efficiency is shown in Fig.10b. When the speed increases from 1000 rpm to 10000 rpm, the efficiency obtained by both methods increases with the speed. The average efficiency under Method I and Method II increased by 0.25 % and 0.4 %, respectively. From Fig. 10c, gear efficiency decreases with increasing surface roughness, by 0.29 % for Method I and 1.59 % for Method II. This indicates that the TFC is highly sensitive to surface roughness, because as the roughness increases, the formation of the lubricating oil film in the gear contact area becomes difficult, leading to an increase in friction losses and a decrease in efficiency. From Fig. 10d, with the increase in lubricating oil temperature, the gear efficiency of Method I decreases by 0.06 %, and the gear efficiency of Method II increases by 1.32 %. The result shows that the AFC is not sensitive to lubricant operating temperature, which is consistent with the results obtained in [33]. When the oil temperature increases, the viscosity of the lubricant decreases, which significantly improves efficiency. However, in Method II, when the oil temperature rises, the viscosity of the lubricant decreases and the efficiency improves significantly. Therefore, in gear design, it is necessary to select a reasonable operating temperature range for the lubricant according to the actual operating conditions, to fully utilize the properties of the lubricant, reduce the frictional power loss of gears, and improve the efficiency of the robot joint reducer.

3.2 Gear Instantaneous Input Torque Under Different Operating Conditions

In this section, the input torque fluctuations due to instantaneous efficiency fluctuations are discussed under constant load torque conditions. Fig. 11a shows

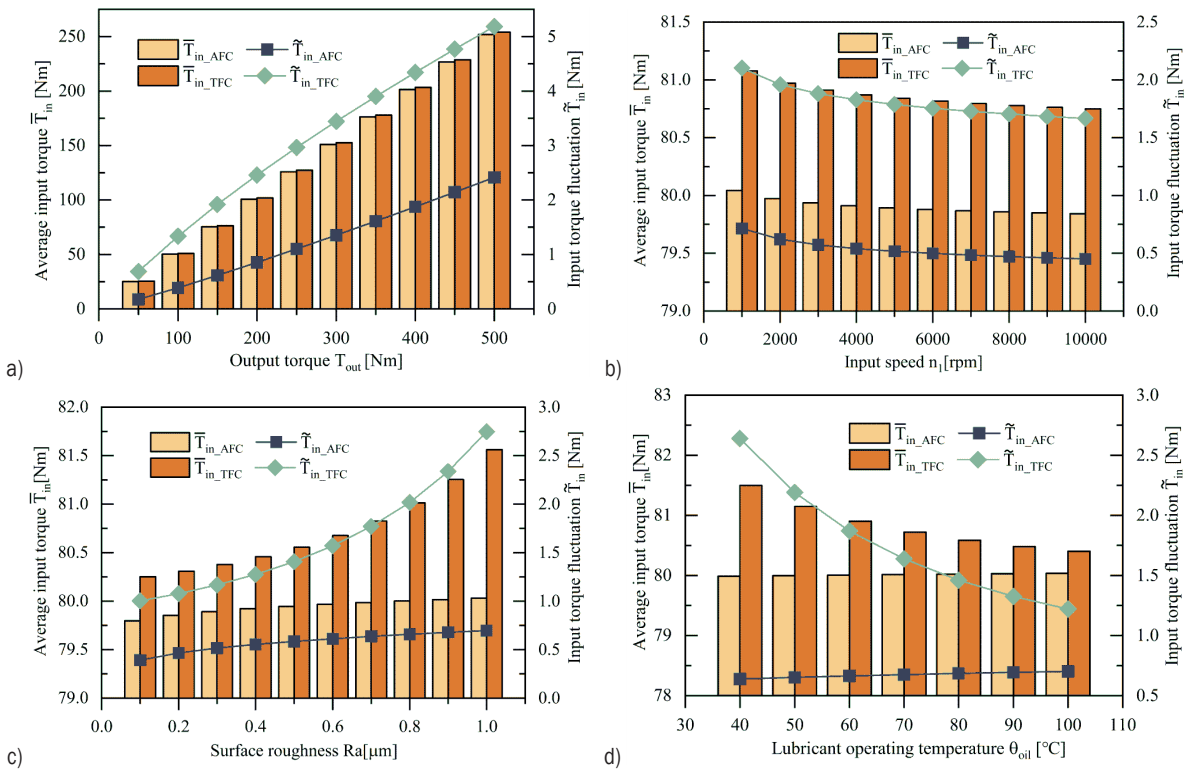

Fig. 11. *Input torque and torque fluctuation of gears; a) at case 2, b) at case 3, c) at case 4, and d) at case 5*

the influence of different output torques on the input torque fluctuations of the gear. T_{in_AFC} and T_{in_TFC} represent the average input torque under Method I and Method II respectively. $\tilde{T}_{in\_AFC}$ and $\tilde{T}_{in\_TFC}$ represent the instantaneous torque fluctuation under Method I and Method II, respectively. It can be seen that when the output torque increases, the torque fluctuation will increase with the increase of output torque, whether the AFC or the TFC is used. Therefore, it is necessary to choose a suitable output torque range according to the actual operating conditions in gear design, to reduce the torque power loss and improve the working smoothly of the robot joint reducer. As Fig. 11b shows, increasing the rpm from 1000 rpm to 1000 rpm reduced torque fluctuation by 36 % and 20 % for Method I and Method II, respectively. Fig. 11c shows that gear input torque fluctuation increases with surface roughness, especially under EHL conditions. Therefore, in design, it is necessary to ensure the smoothness of the gear contact surface as much as possible to promote the formation of oil film on the meshing surface and reduce the torque fluctuation during gear meshing. From Fig. 11d, as the lubricating oil temperature increases from 40 ºC to 100 ºC, the gear input torque fluctuation of Method I increases from 0.64 Nm to 0.70 Nm, and the gear input torque fluctuation of Method II decreases from 2.63 Nm to 1.22 Nm. Under EHL conditions, the lubricating oil operating temperature is one of the important factors affecting gear efficiency and torque fluctuation. As the temperature rises, the viscosity of the lubricating oil decreases, which can reduce the viscous resistance of the oil and improve the meshing efficiency of the gear, thereby reducing the input torque fluctuation.

Through the analysis of gear efficiency and torque fluctuation under the same operating conditions in Figs. 10b and 11b, Figs. 10c and 11c, Figs. 10d and 11d, it was found that regardless of using Method I or Method II, the average input torque of the gear will decrease as the average efficiency increases. At the same time, the input torque fluctuation of the gear increases with the increase of efficiency fluctuation. Therefore, studying the laws of gear efficiency and torque fluctuation is conducive to establishing a more accurate friction model and torque fluctuation compensation method for the joint reducer of collaborative robots.

4 DISCUSSION

The gear transmission efficiency and torque fluctuation are influenced by various factors, including gear output torque, input speed, tooth surface roughness, and temperature, among which the friction coefficient has the greatest impact. In Method I, decreasing the output torque and gear roughness and increasing the input speed can improve gear efficiency, with roughness and speed having the greatest influence on efficiency, while lubricating oil temperature has little effect. In Method II, increasing the output torque, rotational speed, and lubricating oil temperature, and decreasing gear roughness can enhance gear efficiency, with suitable roughness and lubricating oil temperature contributing to around 1.5 % efficiency improvement. The average efficiency calculated by Method I and Method II differs by a maximum of 1.86 %. Under case 4, the instantaneous efficiency variation of the gear can reach 3.34 %. Regarding the input torque fluctuation, both Method I and Method II can reduce the torque fluctuation amplitude by lowering the output torque, and the gear surface roughness, and increasing the speed, resulting in smoother gear operation. In addition, in Method II, raising the lubricating oil temperature can reduce torque fluctuation by 53.6 %. Under case 2, the torque fluctuation of the gear can reach 5.19 Nm. Method I assumes a constant friction coefficient along the meshing line, neglecting the influence of lubricating oil temperature, and is often used to calculate the average efficiency of gears or roughly evaluate gear performance in spur gear transmission design. The friction coefficient of Method II varies along the meshing line and is based on the instantaneous efficiency calculation model presented in this study, so the combination of the two provides a good evaluation of the real-time efficiency at each meshing position in the spur gear pair. For an accurate calculation of the instantaneous efficiency of the gear, the time-varying friction coefficient is recommended in this study.

To evaluate the accuracy of the calculation method proposed in this paper, the numerical results obtained by the present method were compared with those reported in previous studies under the same conditions as described in the reference **[15]**. Table 3 and Fig. 12 presents the factors considered and the corresponding results from the efficiency calculation models described in the literature. The comparison showed that the average efficiency calculated using the present method I was consistent with the results reported by Höhn **[11]** and Diez-Ibarbia et al. **[15]**, with a difference of only 0.01 %. This can be attributed to the fact that the present study did not treat the friction coefficient as a constant but allowed it to vary with the changing contact conditions at different mesh positions, as shown in Fig. 4. Through comparative

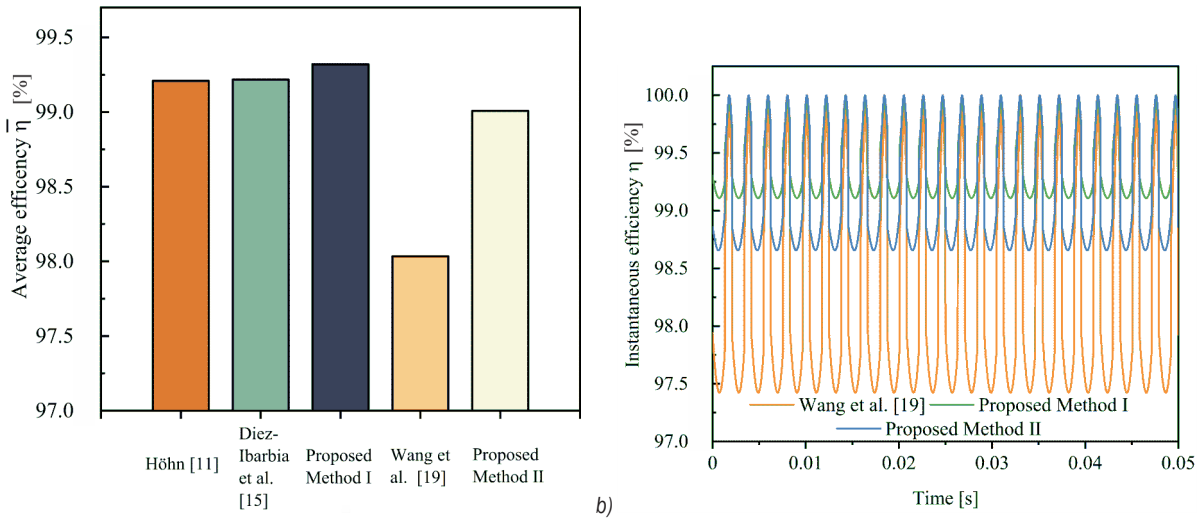

Fig. 12. *Gear efficiency comparison; a) average efficiency under different methods, and b) instantaneous efficiency under different methods*

Table 3. *Comparison of results between different methods under the same conditions*

Method	Instantaneous efficiency	Average efficiency	Method I	Method II	Load distribution	Torque balance	$\bar{\eta}$ [%]
Höhn [11]		✓	✓		✓		99.21
Diez-Ibarbia et al. [15]		✓	✓		✓		99.22
Proposed Method I	✓		✓		✓	✓	99.32
Wang et al. [19]	✓				✓		98.03
Proposed Method II	✓			✓	✓	✓	99.01

symbol ✓: the method has this characteristic.

analysis, the effectiveness and accuracy of the proposed method in this paper have been verified. This paper proposes a more accurate calculation model for the instantaneous efficiency of gear pairs compared to the model proposed in reference [19], by considering the meshing position, load distribution, and both average and time-varying friction coefficient models of the gear pair.

5 CONCLUSIONS

In this paper, through the analysis of the meshing characteristics of the external meshing gear pair, a numerical calculation model for the instantaneous efficiency of the gear is established under the comprehensive consideration of the friction coefficient model, the load distribution model between the teeth and the torque balance of the meshing point. This model can calculate the instantaneous efficiency of the gear and its corresponding input torque fluctuations. Then, two different friction coefficient models are used to compare the change laws of gear instantaneous efficiency and instantaneous input torque along the meshing position under the same operating conditions, and also studies the changing law of gear efficiency and efficiency fluctuation, input torque and input torque fluctuation under different load, speed, roughness, and temperature conditions. The following conclusions can be drawn:

- The instantaneous efficiency of gears in the double-tooth meshing area is lower than that in the single-tooth meshing area. Ensuring continuous and stable transmission of gears, the gear transmission efficiency can be improved by reducing the degree of contact ratio.
- Different friction coefficient models have a significant impact on the efficiency and efficiency fluctuation of gears. The efficiency calculated using the time-varying friction coefficient model is lower than that calculated using the average friction coefficient model, and the maximum difference between the two is 1.86 %. In contrast, the value of the torque fluctuation under the average friction coefficient is smaller than that under the time-varying friction coefficient.
- The instantaneous efficiency of the gear increases and the instantaneous input torque decreases under constant load. The gear efficiency

fluctuation increases, and the torque fluctuation at the input end also increases. Under specific operating conditions, the gear pair's instantaneous efficiency variation can reach 3.34 %, and the torque fluctuation can reach 5.19 Nm.

- Increasing the input speed, raising the operating temperature of the lubricating oil, and reducing the surface roughness of the gear can improve the gear transmission efficiency and reduce the torque fluctuation during meshing. In addition, an increase in output torque will increase the torque fluctuation.

This paper presents numerical calculations of the instantaneous efficiency and torque fluctuation of an external meshing gear pair using theoretical analysis. Some of the computed results are consistent with previous studies. However, the presented model only considered the instantaneous efficiency and torque fluctuation of gears under sliding friction, while neglecting the effects of rolling friction losses and non-load-related losses on gear efficiency and torque fluctuation. In addition, the precision and manufacturing errors of gear are also ignored. Therefore, experimental verification of the model is still necessary in future research. Additionally, the development of a model for the instantaneous efficiency and torque fluctuation of a cooperative robot joint reducer composed of gear pairs will be the focus of our future research.

6 ACKNOWLEDGEMENTS

This work is supported by the National Natural Science Foundation of China (Grant No. 92048201). The authors thank the reviewers for their valuable comments on the manuscript.

7 REFERENCES

[1] Akiyama, N., Fujimoto, Y. (2019). Highly efficient 2K-H compound planetary reduction gearbox using balancer. *45th Annual Conference of the IEEE Industrial Electronics Society*, p. 669-674, **DOI:10.1109/IECON.2019.8926722**.

[2] Kanai, Y., Fujimoto, Y. (2019). Performance analysis of torque-sensorless assist control of a powered exoskeleton using highly back-drivable actuators. *IEEE 17th International Conference on Industrial Informatics*, p. 577-582, **DOI:10.1109/INDIN41052.2019.8972220**.

[3] Zhang, H., Ahmad, S., Liu, G. (2015). Modeling of torsional compliance and hysteresis behaviors in harmonic drives. *IEEE/ASME Transactions on Mechatronics*, vol. 20, no. 1, p. 178-185, **DOI:10.1109/tmech.2014.2311382**.

[4] Matsuki, H., Nagano, K., Fujimoto, Y. (2019). Bilateral drive gear-a highly backdrivable reduction gearbox for robotic actuators. *IEEE/ASME Transactions on Mechatronics*, vol. 24, no. 6, p. 2661-2673, **DOI:10.1109/tmech.2019.2946403**.

[5] Brassitos, E., Kong, Q., Mavroidis, C., Weinberg, B. (2014). Design improvements and design methodology for the gear bearing drive: A compact, powerful and cost-effective robotic actuator. *Proceedings of the ASME 2014 International Design Engineering Technical Conferences and Computers and Information in Engineering Conference*, vol. 5B: 38th Mechanisms and Robotics Conference, p. 17-20, **DOI:10.1115/DETC2014-35377**.

[6] Kanai, Y., Fujimoto, Y.. (2018). Torque-sensorless control for a powered exoskeleton using highly back-drivable actuators. *44th Annual Conference of the IEEE Industrial Electronics Society,* p. 5116-5121, **DOI:10.1109/IECON.2018.8591255**.

[7] Pham, A.-D., Ahn, H.-J. (2018). High precision reducers for industrial robots driving 4th industrial revolution: State of arts, analysis, design, performance evaluation and perspective. *International Journal of Precision Engineering and Manufacturing-Green Technology*, vol. 5, p. 519-533, **DOI:10.1007/s40684-018-0058-x**.

[8] Kobuse, D., Fujimoto, Y. (2016). Efficiency optimization of high-reduction-ratio planetary gears for very high power density actuators. *IEEE 25th International Symposium on Industrial Electronics*, p. 1240-1245, **DOI:10.1109/ISIE.2016.7745072**.

[9] Qiu, Z., Xue, J. (2021). Review of performance testing of high precision reducers for industrial robots. *Measurement*. vol. 183, art. ID 109794, **DOI:10.1016/j.measurement.2021.109794**.

[10] Brassitos, E., Jalili, N. (2020). Dynamics of integrated planetary geared bearings. *Journal of Vibration and Control*, vol. 26, no. 7-8, p. 565-580, **DOI:10.1177/1077546319889848**.

[11] Höhn, B.-R. (2010). Improvements on noise reduction and efficiency of gears. *Meccanica*, vol. 45, p. 425-437, **DOI:10.1007/s11012-009-9251-x**.

[12] Baglioni, S. Cianetti, F., Landi, L. (2012). Influence of the addendum modification on spur gear efficiency. *Mechanism and Machine Theory*, vol. 49, p. 216-233, **DOI:10.1016/j.mechmachtheory.2011.10.007**.

[13] Pleguezuelos, M., Pedrero, J.I., Sánchez, M.B. (2013). Analytical expressions of the efficiency of standard and high contact ratio involute spur gears. *Mathematical Problems in Engineering*, vol. 2013, Art. ID 142849, **DOI:10.1155/2013/142849**.

[14] Marques, P.M.T., Martins, R.C., Seabra, J.H.O. (2016). Power loss and load distribution models including frictional effects for spur and helical gears. *Mechanism and Machine Theory*, vol. 96, p. 1-25, **DOI:10.1016/j.mechmachtheory.2015.09.005**.

[15] Diez-Ibarbia, A., del Rincon, A.F., Iglesias, M., de-Juan, A., Garcia, P., Viadero, F. (2016). Efficiency analysis of spur gears with a shifting profile. *Meccanica*, vol. 51, p. 707-723, **DOI:10.1007/s11012-015-0209-x**.

[16] Diez-Ibarbia, A., Fernandez-Del-Rincon, A., Garcia, P., De-Juan, A., Iglesias, M., Viadero, F. (2018). Assessment of load dependent friction coefficients and their influence on spur gears efficiency. *Meccanica*, vol. 53, p. 425-445, **DOI:10.1007/s11012-017-0736-8**.

[17] Diez-Ibarbia, A., Fernandez-del-Rincon, A., de-Juan, A., Iglesias, M., Garcia, P., Viadero, F. (2018). Frictional power

losses on spur gears with tip reliefs. The friction coefficient role. *Mechanism and Machine Theory*, vol. 121, p. 15-27, **DOI:10.1016/j.mechmachtheory.2017.10.003**.

[18] Petry-Johnson, T.T., Kahraman, A., Anderson, N.E., Chase, D.R. (2008). An experimental investigation of spur gear efficiency. *Journal of Mechanical Design*, vol. 130, no. 6, art. ID 0626101, **DOI:10.1115/1.2898876**.

[19] Wang, A., Gitnes, S., El-Bayoumy, L. (2011). The instantaneous efficiency of epicyclic gears in flight control systems. *Journal of Mechanical Design*, vol. 133, no. 5, art. ID 051008, **DOI:10.1115/1.4004001**.

[20] Cao, W., He, T., Pu, W., Xiao, K. (2021). Dynamics of lubricated spiral bevel gears under different contact paths. *Friction*, vol. 10, p. 247-267, **DOI: 10.1007/s40544-020-0477-x**.

[21] Li, S., Kahraman, A. (2010). Prediction of spur gear mechanical power losses using a transient elastohydrodynamic lubrication model. *Tribology Transaction*s, vol. 53, no. 4, p. 554-563, **DOI:10.1080/10402000903502279**.

[22] Xu, H., Kahraman, A., Anderson, N.E., Maddock, D.G. (2007). Prediction of mechanical efficiency of parallel-axis gear pairs. *Journal of Mechanical Design*, vol. 129, no. 1, p. 58-68, **DOI:10.1115/1.2359478**.

[23] Raviola, A., Guida. R., De Martin, A., Pastorelli, S., Mauro, S., Sorli, M. (2021). Effects of temperature and mounting configuration on the dynamic parameters identification of industrial robots. *Robotics*, vol. 10, no. 3, art. ID 83, **DOI:10.3390/robotics10030083**.

[24] Tadese, M., Pico, N., Seo, S., Moon, H. (2022). A two-step method for dynamic parameter identification of Indy7 collaborative robot manipulator. *Sensors*, vol. 22, no. 24, art. ID 9708, **DOI:10.3390/s22249708**.

[25] Okorn, I., Nagode, M., Klemenc, J. (2021). Operating Performance of External Non-Involute Spur and Helical gears: A review. *Strojniški vestnik - Journal of Mechanical Engineering*, vol. 67, no. 5, p. 256-271, **DOI:10.5545/sv-jme.2020.7094**.

[26] Piccoli, M., Yim, M. (2016). Anticogging: Torque ripple suppression, modeling, and parameter selection. *The International Journal of Robot*. vol. 35, no. 1-3, p. 148-160. **DOI:10.1177/0278364915599045**.

[27] Lu, Y., Lin, S., Hauschild, M., Hirzinger, G. (2012). A torque-ripple compensation scheme for harmonic drive systems. *Electrical Engineering*, vol. 95, p. 357-365, **DOI:10.1007/s00202-012-0264-4**.

[28] Fernandes, C.M.C.G., Marques, P.M.T., Martins, R.C., Seabra, J.H.O. (2015). Gearbox power loss. Part II: Friction losses in gears. *Tribology International*, vol. 88, p. 309-316, **DOI:10.1016/j.triboint.2014.12.004**.

[29] Sánchez, M.B., Pleguezuelos, M., Pedrero, J.I. (2017). Approximate equations for the meshing stiffness and the load sharing ratio of spur gears including hertzian effects. *Mechanism and Machine Theory*, vol. 109, p. 231-249, **DOI:10.1016/j.mechmachtheory.2016.11.014**.

[30] Miler, D., Hoić, M. (2021). Optimisation of cylindrical gear pairs: A review. *Mechanism and Machine Theory*, vol. 156, art. ID 104156, **DOI:10.1016/j.mechmachtheory.2020.104156**.

[31] ISO/TR 14179-2:2001. Gears - Thermal capacity - Part 2: Thermal load carrying capacity. International Standard Organization, Geneva

[32] Hammami, M., Martins, R., Abbes, M.S., Haddar, M., Seabra, J. (2017). Axle gear oils: Tribological characterization under full film lubrication. Tribology Internationa, vol. 106, p. 109-122, **DOI:10.1016/j.triboint.2016.05.051**.

[33] Fernandes, C.M.C.G., Martins, R.C., Seabra, J.H.O. (2016). Coefficient of friction equation for gears based on a modified Hersey parameter. *Tribology Interntional*, vol. 101, p. 204-217, **DOI:10.1016/j.triboint.2016.03.02**.